IDENTIFICATION OF LIQUEFACTION FAILURES BASED ON AERIAL IMAGES

J.A. Buchheister[1] and M. Rezaeian[2]

[1] *PhD student, Dept. of Civil, Environmental and Geomatic Engineering, Institute for Geotechnical Engineering, ETH Zurich. Switzerland*
[2] *PhD student, Dept. of Civil, Environmental and Geomatic Engineering, Institute of Geodesy and Photogrammetry, ETH Zurich. Switzerland*
Email: juliane.buchheister@igt.baug.ethz.ch, mehdi.rezaeian@geod.baug.ethz.ch

ABSTRACT :

One helpful tool to detect damages after an earthquake in cities is images analysis. Aerial images can be taken before and after an earthquake. By comparing both images it is possible to analyze the damages that are caused by the earthquake event. It is important to find out as soon as possible where the biggest damage to structures and lifelines has happened in order to start immediate help and reduce further risk. Especially in urban areas the analysis of the damage defines the remedial action.

Certain damages can be referred clearly to the soil such as large ground deformations, ground failures or lateral spreading. One of the reasons is soil liquefaction. Based on soil-structure interaction, liquefaction can cause severe damage e.g. tilting and sinking of buildings next to sand volcanoes. Aerial photogrammetry, satellite images and SAR laser profiling data are utilized to supply many opportunities for determination of ground displacement and liquefaction failures depending on resolution and measuring accuracy.

In this paper, first soil liquefaction and photogrammetric measures are explained, second, the process of analyzing the images with focus on building damage associated with liquefaction failure is described and third the knowledge is applied on a case study in Adapazari after the 1999 Kocaeli earthquake. Especially in the old city centre numerous liquefaction events were reported. Aerial images are available before and after the earthquake as well as soil information based on borings.

KEYWORDS: Liquefaction, aerial image, photogrammetry, soil-structure interaction, damage, case study

1. INTRODUCTION

After an earthquake the damage to structures is of big concern. The main influence factor (e.g. type of structure, ground failure, others) should be detected after classifying the damage. This is relevant to decide on the right remedial action. Certain damages on buildings can be related directly to ground failure (Kiku et al. 2001).

More and more air and space-borne images are used after a catastrophic event such as an earthquake to estimate and grasp damage situations without depending on information sent from the interiors of the damaged area. In the case that pre-event imagery data exist it is a great advantage. The challenge is to replace visual interpretation of optical remote sensing images, accomplished by expert photo-interpreters, with automatic or semi-automatic classification techniques. Using advanced methods of digital image processing, a first assessment of the extent of the damage can be made (Rezaeian and Gruen, 2007). The basis for these methods is a multi-tiered procedure that allows broad regional damage assessments to be conducted using moderate-resolution data (from satellites e.g. SPOT, ALOS/PRISM, Cartosat-1) and more detailed assessments using high-resolution information (from satellites e.g. QuickBird, IKONOS). In the following contribution we concentrate on the damage that is related to the soil.

We emphasis soil liquefaction as the type of soil failure that causes the biggest damage of soil failures. Slope failures are not regarded. The procedure will be illustrated by a case study in the city Adapazari in Turkey after the 1999 Kocaeli earthquake. The area of the case study is mainly flat that means a height difference less than 5m over an area of 1km x 1km. For such a case study different types of data have to be available: specific ground information and good quality images. One study from Tomatsu and Sato (1996) on the identification of liquefaction failures from images was carried out in Japan but lacking on good soil and image information especially in the densely covered area as for example cities.

1.1. Introduction to soil liquefaction

Soil liquefaction is defined as the soil changes from a solid to a liquid state mainly during excitation e.g. an earthquake. The consequences of soil liquefaction can be noticed considerably at a structure. The structure tilted or/and settled not uniformly. In Figure 1 the building shows an enormous inclination due to the rotation of the whole building and settles more at one side than at the other. Other consequences of soil liquefaction that happen in the free field are sand volcanoes and sand boils. Usually the damage in the free field e.g. on agricultural land is limited such as sand spread over the fields combined with small settlements. Whereas the damage to structures e.g. buildings can be severe. Both indices are clearly visible as phenomena of soil liquefaction.

a b

Figure 1: (a) Tilted and settled building in Adapazari (Peer 2000), (b) sketch of liquefaction underneath a building (Buchheister 2007)

The presence of saturated and loose sandy silty soil is a specific precondition for the susceptibility to soil liquefaction. Usually the ground water table is close to the surface in order to find saturated soil layers. The necessary soil information can be retrieved from microzonation maps. More soil information is found from actual boring data. Sometimes detailed soil information from laboratory tests is available. Seldom former liquefied areas are known. The better the quality of soil information the better is the accuracy for assessing soil liquefaction. Based on a possible earthquake magnitude the liquefaction susceptibility is assessed e.g. by using the simplified procedure (latest findings in Youd et al., 2001).

Actual research shows that the influence of liquefaction on a structure is not clear. The liquefaction potential under a structure is higher than in the free field especially for periods of 0.6-0.7 seconds, e.g. six story structures (Soyoz et al., 2007). When the soil softens through the earthquake loading e.g. by soil liquefaction the softened soil can isolate the seismic demand on the structure (Pitilakis et al., 2006). Since soil-structure interaction is not fully understood aerial images are a helpful tool to evaluate damages based on soil failures.

Soil-structure interaction plays an important role as every structure is founded on soil. The load of each structure is transferred into the upper ground directly underneath the structure, called the subsoil. This subsoil consists of different layers of soil. As soon as one of these layers fails due to the earthquake loading the structure can settle, rotate or translate consequently. Damage is caused to the structure depending on the magnitude of soil and structure movements.

1.2. Introduction to Aerial Images

Aerial photogrammetry and remote sensing include techniques of measuring objects from photographs, which cover a broad area. Remote sensing technique (either by space-borne or air-borne sensors) was employed in the last decades to detect, identify and monitor the impact and effects of natural disasters like earthquakes, landslides and floods. Optical sensors are widely used in damage observation and assessment. Optical images are easy to interpret as they present the ground surface as it appears to the human eye. Damage survey at the level of individual buildings is more successful with the use of very high-resolution images.

Aerial imagery can be obtained in a much more controlled fashion, both in terms of time and flight planning (data acquisition pattern) and with much higher geometric, spectral and radiometric resolution. In addition, real-time and on-line processing capabilities with digital images are available. Stereoscopic aerial photos provide the possibility to access geometric information of a wide damaged area. The domain of aerial photogrammetry for conclusions based on geometrical measurements is confined by resolution and measurement accuracy. The planimetric accuracy is directly proportional to the image scale, whereas altimetry accuracy is proportional to the flying height. For targeted and very well defined points, an estimation of the planimetric accuracy is about one-third of the terrain pixel size (typically 5-10 centimeters) and the altimetry accuracy is 2 to 3 times (equivalent to 10-30 centimeters). With stereoscopic aerial photos structure geometry, individual buildings and also slope movements are obtained.

In this study, a data set from the Adapazari, Turkey earthquake was used. It includes a B/W stereo pair of aerial photos before and after the earthquake. The pre-event aerial imagery dates from 1994 at scale 1:35000 and the post-event images dates from 1999 at scale 1:18000 (Figure 2). A Digital Surface Model (DSM) is created automatically from the aerial images. The key problem of DSM generation is the stereo image matching. Basically, automatic image matching is a challenging process, thus no perfect algorithm could be developed yet.

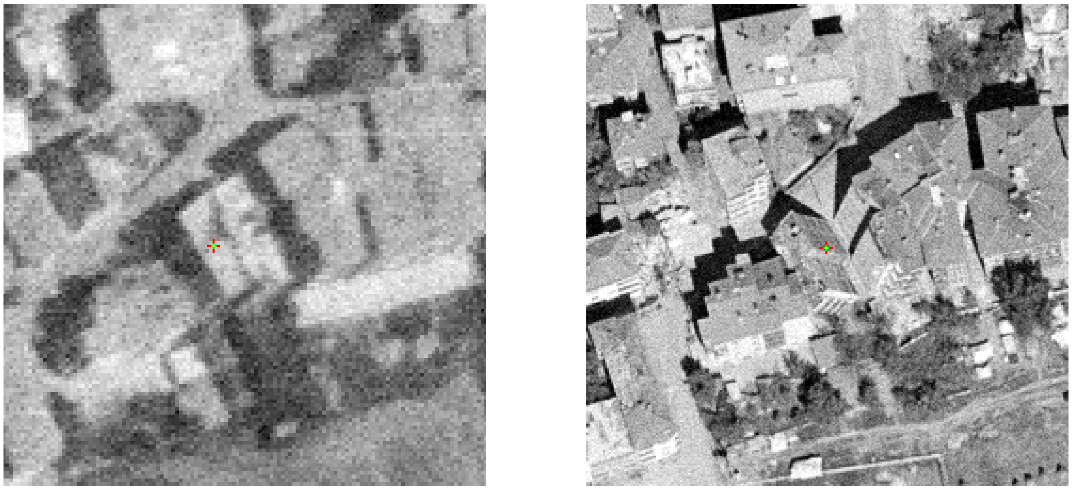

(a) Before the earthquake (b) After the earthquake

Figure 2: Two pairs of aerial images before (1994) and after(1999) of Adapazari earthquake –Turkey (Scale 1: 35000 & 1:18000 Grayscale image)

Visual photo-interpretation analysis is a reliable technique for earthquake damage assessment. According to the performed studies, damage identification via space/airborne images is restricted to some type of visible changes, categories like: totally or partially collapsed (severely damaged), tilted and overturned building, displacement of building appendices, split in the middle of high-rise building and debris. For this purpose, a visual inspection of building damages was conducted, based on stereo pairs of aerial photos before and after the earthquake. A multilevel damage scale (collapsed, partially collapsed, overturned, inclined, no damage) appears to be adequate in representing the distribution of individual building damages. Overturned and inclined buildings can be used as indicators for soil liquefaction.

2. CORRELATIONS OF VISUAL DAMAGES

Table 1 gives an extensive overview about the classification of visual damages. Typical damages due to liquefaction are accordingly: inclination, inclined plane, overturn collapsed and pancake collapse. The pancake collapse and the inclined plane are only related to soil liquefaction when the ground floor settles as well. Concerning these cases the image analysis shows a lack of describing the whole damage of a building. Inclination is mostly related to softening of the soil such as the phenomenon of liquefaction but can be as well failure of the supporting construction in the lower floors. The overturn of a building is only possible by tremendous liquefaction. Often another building stops the turning of a building.

Table 1: Damage types proposed by Schweier and Markus (2004).

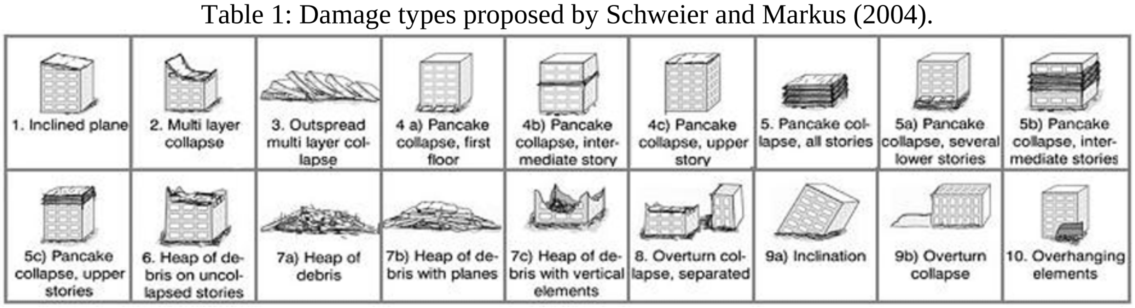

Another possibility to describe the damage is the classification according to the European Macroseismic Scale 1998 (EMS-98, Grunthal, 1998). Therein damage grades of masonry and reinforced concrete buildings are defined. The grades are based on structural and non-structural damage. Pancake collapse and overturn is classified in the highest damage grade 5, meaning destruction. Inclined plane equals damage grade 4, meaning very heavy damage. Inclination falls in the range of damage grade 1 to 3, meaning negligible to heavy damage, as the inclination due to liquefaction reduces the structural damage. But the degree of tilt can make the living in the inclined building impossible. Buildings that reach settlements greater than 1/150 of the shorter building length based on angular rotation are already expected to have cracks and fissures as building damage (after Bjerrum in Smoltczyk 1996). This equals an inclination of 0.4 degrees. In terms of the intensity that includes little to heavy damages on structures equals intensity grades VI to VIII.

To classify ground failure more detailed in an engineering way Table 2 is very helpful. The settlements and tilts could be diffracted by the images. Herein the accuracy of measurements should be at least 10cm for vertical settlements and 1cm to derive differential settlements. The accuracy of 1cm can be reached only by terrestrial photogrammetry.

Table 2: Ground failure index classification system (Bray et al. 2000). Δ = differential settlement

Index	Description	Interpretation
GF0	No observable ground failure	No vertical movement, tilt, lateral movement, or boils
GF1	Minor ground failure	Vertical movements, $\Delta < 10$ cm; tilt of > three-storey buildings $< 1°$; no lateral movements
GF2	Moderate ground failure	$10 < \Delta < 25$ cm; tilts of 1–3°; small lateral movements (< 10 cm)
GF3	Significant ground failure	$\Delta > 25$ cm; tilts of > 3°; lateral movements > 25 cm

3. ANALYSIS OF DAMAGE CAUSED BY LIQUEFACTION IN ADAPAZARI

The Kocaeli earthquake 1999 caused immense damage in the area east of Istanbul (Sakarya) e.g. as described in an extensive report about the earthquake by USGS (2000). In the city of Adapazari the damage in the centre can be directly related to liquefaction. The authors identified 11 buildings that correlate with liquefaction phenomena. A similar result as Bray et al. (2001) who found twelve sites settled or tilted due to liquefaction or ground softening. In Figure 3 the available boring information and the damaged buildings related to soil liquefaction is presented.

The pre- and post-event photographs (shown in Figure 2) were scanned at 21-micron pixel size, giving footprints of 74 cm and 38 cm on the object, respectively. Calibration reports of the camera and ground control points were available and used as input information for orientation procedures. Moreover, a digital two-dimensional vector (planimetric) map from a part of the damaged area was available. In this study DSM created at 2m spatial resolution using the DSM tool of VirtouZo software (Supersoft ver 3.3). Using this DSM, average height values of each region - enclosed by building polygons - were assigned to polygon vertices as z-values and then refined manually having the best possible measurement accuracy.

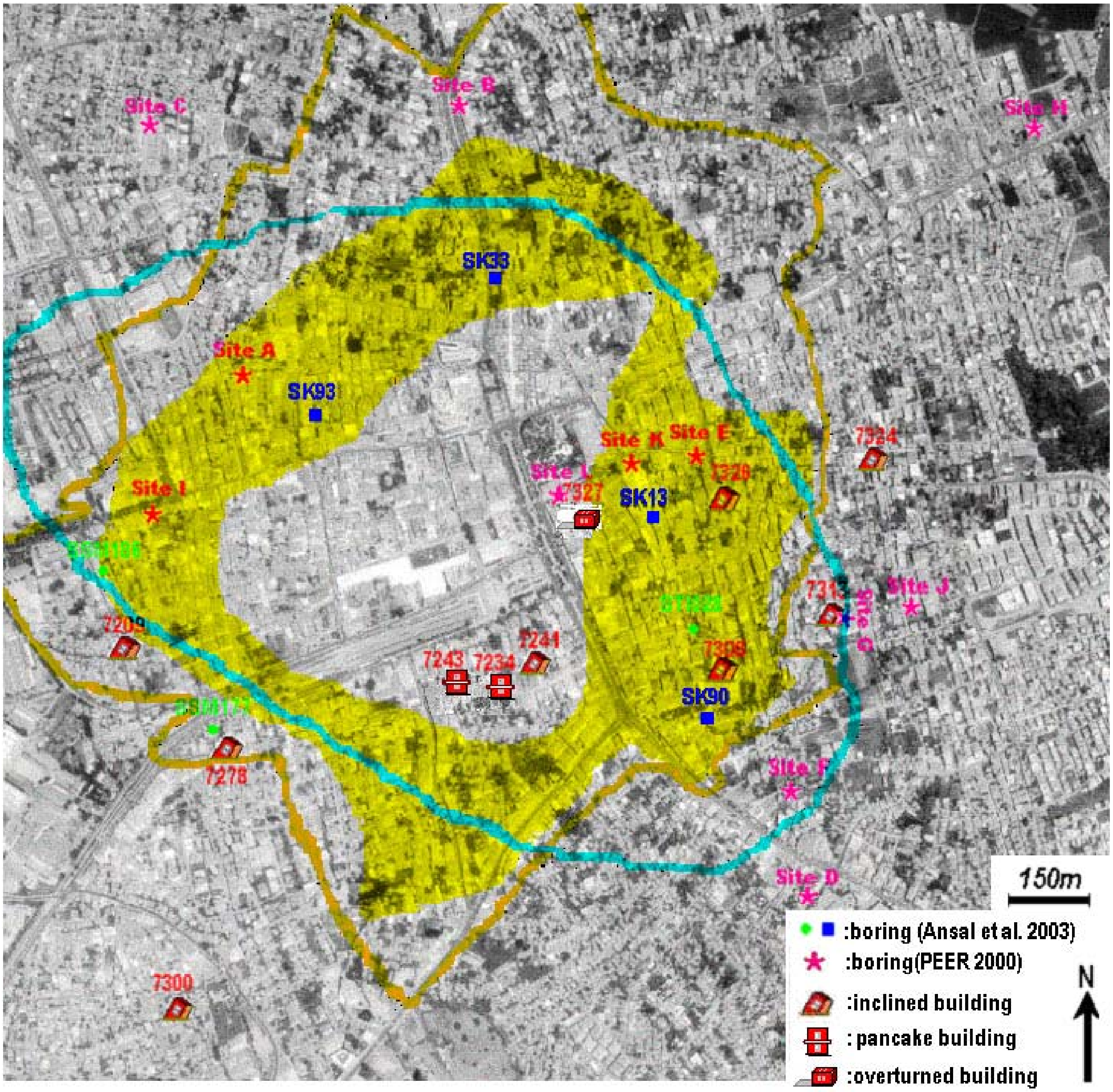

Figure 3: Aerial image indicating boring information and damaged buildings related to soil liquefaction in Adapazari city centre, Turkey (yellow lines=research area and yellow fill=liquefied area after Yasuda, 2004, blue circle=15%-30% collapsed or heavily damaged buildings and the 33%-67% presence of silt and sand layer after Bakir et al., 2002)

Yasuda (2004) defined a research area in Adapazari (yellow lines in Figure 3) that is affected only by liquefaction (area filled yellow in Figure 3). Bakir et al. (2002) found that inside their investigated area (blue lines in Figure 3) 15% to 30% of the buildings are collapsed and heavily damaged. The authors showed that the amount of sand and silty sand in the described boreholes is equivalent to 33% to 67%. This high ratio indicates a high liquefaction potential of the prevalent soil layers as the ground water level is only several meters below the ground surface that means those layers are presumably saturated. It stands out that a connection could be made between the damaged buildings and liquefaction prone soil layers in the described area.

Table 3: Summary of the 11 damaged buildings, - coordinate information ruined, * one corner measurements is missing, (negative settlement) uplift

Building Nr.	Height (m)	Av. Footprint (m^2)	Av. Settlement (m)	Max. Settlement (m)	Max. Tilt (°)	Damage Tab.1	Damage Tab.2
7209	14.5	95	0.72	4 (-1)	29.4	9a	GF3
7234	31.1	-	4.67*	5	1.8	4, 5	GF2-3
7241	11.0	218	2.6	4.5	9.3	9a	GF3
7243	12.0	449	5.45	6.8	3.6	4, 5	GF3
7278	11.8	235	2.18	5.4	29.0	9a	GF3
7300	12.0	153	0.98	2.1 (-1.3)	12.7	9a	GF3
7308	12.3	300	4.08	6	7.9	9b	GF3
7313	11.0	351	2.1	4.5	8.8	9a	GF3
7324	13.0	426	2.48	3.4	9.6	9a	GF3
7326	13.0	-	4.97*	7.7	15.0	9a	GF3
7327	12.0	-	-	-	-	9b	-

In Table 3 the result of the study is summarized. These buildings have a height ranging from 11 to 14.50m equivalent to 4-5 stories buildings. The footprint ranges from $95m^2$ to $449m^2$, which is typical for apartment buildings. The footprint is calculated from the main corners of the building frame (object extracted before the earthquake). The maximum inclination is determined mostly over the diagonal of the rectangular building area. Some inaccuracy in the calculation is possible as the corner points of the buildings are on the roof and the building objects show no right corners. The height is averaged from the corner points of the building to the street. The accuracy of the vertical measurements is 78cm and the horizontal measurement is 38cm due to the quality of the available image as mentioned before.

Three pairs of aerial image and soil information are discussed:

1. *Three borings at site K and E and sk13 and two buildings 7327 and 732*6. All borings show liquefaction prone layers. Building 7326 tilted (Damage classification 9a after Table 1) and 7327 overturned (Damage classification 9b after Table 1) due to soil liquefaction in the zone identified as the area with numerous liquefaction failures. Unfortunately, the coordinates of the corner points of building 7327 could not be detected after the earthquake. Building 7326 has a maximum differential settlement of 4.97m +/- 78cm of accuracy and a maximum inclination of 15 degrees. According to the coordinates of the corner of the building a rotation is noticed after the earthquake, which is not discussed in the used classification of damaged buildings. The building not only settled vertically and tilted but also translated and rotated. Both buildings are classified as ground failure type GF3 after Table since the tilt and differential settlements are major.
2. *Two borings SSM177 and SSM 186 and buildings 7278 and 7209*. Both borings show layers of silt and low plasticity clay and silt that give a safety factor smaller of 1 in a depth of 2.2-7.2m. Both buildings show an inclination of approximately 29 degrees indicating an overturn or another type of damage that cannot be identified by the image clearly. On one hand liquefaction is possible according to the borings but on the other hand the inclination of the buildings based on the aerial photos is not clear. According to the liquefaction zone, no liquefaction failure is expected here but the buildings are very close to the boarder of this area. In terms of the near distance from the building to the boring the building damage can be also due to liquefaction.
3. *Boring G2 from site G and building 7313*. Here the boring is very close to the building, which is a huge advantage in terms of accuracy. The building 7313 inclined by maximum 8.8 degrees and shows differential settlement of 4.2m +/-78cm. Concluding this building shows liquefaction failure even though it lays outside the investigated area of other authors.

The measurements of vertical displacements as summarized in Table are of large magnitude. Some influence might be the difficult detection of the buildings before the earthquake due to the low resolution. Still this size of settlements follows tremendous damage. Typical settlements in the liquefied area are 20 cm to 40 cm and an inclination of 1 to 3 degrees identified by Yasuda et al. (2001). All identified buildings fitted to a liquefaction prone layer in a boring in the vicinity. Visual phenomena of liquefaction failure and liquefaction prone soil layers let conclude a high potential of damage due to liquefaction for all 11 buildings identified.

4. CONCLUSIONS

Following conclusions can be drawn:

1. Building damage due to liquefaction failure can be identified based on aerial images. Helpful tool here is the damage catalogue of buildings of Schweier & Markus (2004) even though it describes soil-structure interaction failures not completely. Damage classification that also takes translation and (planimetric) rotation of buildings into account would be useful to better describe soil failures. For less tremendous damage the classification specialized for ground failures of Bray et al. (2001) can be used. The only handicap might be that the group of people involved in visual damage detection should be very interdisciplinary and object interpretation should be done by professional operators.
2. The damage on buildings is interpreted completely visually and the geometrical measurements are derived from the extracted building objects of the image. More accurate images are needed to better quantify vertical measurements especially differential settlements. This can be reached by large-scale aerial images (e.g. image scale 1:4000). Thus, a purely visual approach is followed to identify liquefaction failures.
3. Some uncertainty remains in building damage detection directly related to liquefaction failure. Inclined, settled, translated and/or rotated building could also include structural failures. Terrestrial images help to exclude failures e.g. that are based on the supporting construction in the lower floors and could be misinterpreted when only interpreted from the sky view.
4. The optimum of identifying liquefaction failures would be a survey focusing on soil failures in the area after the earthquake and have reconnaissance reports with notification of sand boils adjacent to a building as indices for liquefaction. Best soil information quality is needed to assess liquefaction prone layers. Soil classification is mostly sufficient for the subsoil, i.e. mostly up to a depth of 15m depending on the size of the structure.
5. In our case study in Adapazari we experienced a good coherence between liquefaction prone layers in borings and inclined building damage. The borings and images of inclined buildings were within an acceptable distance.

5. ACKNOWLEDGEMENTS

This research developed from the project “Management of Earthquake Risks using Condition Indicators (MERCI)”. The project is funded by the Swiss National Science Foundation (SNF) and ETH Zurich. The authors would like to take the opportunity to thank them all for their support.

REFERENCES

Ansal, A., Springman, S., Studer, J., Demirbas, E., Oenalp, A., Erdik, M., Giardini, D., Sesetyan, K., Demircioglu, M., Akman, H., Fäh, D., Christen, A., Laue, J., Buchheister, J., Cetin, K.O., Siyahi, B., Fahjan, Y., Gülkan, P., Bakir, S., Lestuzzi, P., Elmas, M., Köksal, D. and Gökce, O. (2003). Project Microzonation for Earthquake Risk Mitigation (MERM), Part 2C - Case Studies Microzonation of Pilot Areas: Adapazari, Gölcük, Ihsaniye and Degirmendere. World Institute for Disaster Risk Management (DRM).

Bakir, S., Sucuoglu, H. and Yilmaz, T. (2002). An Overview of Local Site Effects and the Associated Building Damage in Adapazari during the 17 August 1999 Izmit Earthquake. *Bulletin of the Seismological Society of America (BSSA)* **92:1,** 509-526.

Bray, J. D., Sancio, R. B., Durgunoglu, H.T.,Oenalp, A., Seed, R. B., Stewart, J.P., Youd, T. L., Baturay, M. B., Cetin, K. O., Christensen, C., Karadayilar, T. and Emrem, C. (2001). Ground Failure in Adapazari, Turkey. XV ICSMGE TC4 Satellite Conference on "Lessons Learned from Recent Strong Earthquakes". Istanbul, Turkey.

Bray, J.D., Stewart, J.P., Baturay, M.B., Durgunoglu, T., Onalp, A., Sancio, RB. and Ural D. (2000). Damage patterns and foundation performance in Adapazari. Chapter 8 of the Kocaeli, Turkey Earthquake of August 17, 1999.EERI. *Reconnaissance report in Earthquake Spectra Suppl A*, **16,** 163–89.

Buchheister, J. (2007). Soil Liquefaction under Earthquake Loading. PosterNr. HazRi 9. Research Frontiers in Environment and Sustainability. Latsis Symposium. ETH Zurich. Switzerland

Grunthal, G. (1998). European Macroseismic Scale 1998 EMS-98, European seismological Commission, Luxemburg.

Kiku, H.,Yoshida, N., Yasuda, S., Irisawa, T., Nakazawa, H., Shimizu, Y., Ansal, A, and Erken, A. (2001). In-situ Penetration Tests and Soil Profiling in Adapazari, Turkey. XV ICSMGE TC4 Satellite Conference on "Lessons Learned from Recent Strong Earthquakes". Istanbul, Turkey.

Pitilakis, D., Lopez-Caballero, F., Modaressi, A. and Clouteau, D. (2006). Mitigation of existing structures using a "Soft-Caisson"-numerical modelling. First European Conference on Earthquake Engineering and Seismology (1ECEES). Switzerland.

PEER. (2000). Research Turkey Ground Failure (August 1999 earthquakes) Database. http://peer.berkeley.edu/publications/turkey/adapazari/.

Rezaeian, M. and Gruen, A. (2007). Automatic classification of collapsed buildings using object and image space features. In: J. Li, S. Zlatanova and A. Fabbri eds. *Geomatics solutions for Disaster Management.* Springer, 135-148.

Schweier, C. and Markus, M. (2004). Assessment of the search and rescue demand for individual buildings. *Proceedings of the 13th World Conference on Earthquake Engineering*, Vancouver, Canada. Paper No. 3092.

Smoltczyk, U. (1996). Grundbautaschenbuch Teil 1. Ernst und Sohn. Berlin, Germany. (in german).

Soyoz, S., Cetin, K.O. and Sucuoglu, H. (2007). Effects of soil-structure interaction and base isolation on seismic performance of foundation soils. Proceedings of the 4th International Conference on Earthquake Geotechnical Engineering (ICEGE). Greece.

USGS (2000). Implications for Earthquake Risk Reduction in the United States from the Kocaeli, Turkey, Earthquake of August 17, 1999. U.S. Department of the Interior: Babbitt, Bruce and the U.S. Geological Survey: Groat, Charles G. Denver, United States of America.

Yasuda, S., Yoshida, N. and Irisawa, T. (2001). Settlement of buildings due to liquefaction during the 1999 Kocaeli earthquake. XV ICSMGE TC4 Satellite Conference on "Lessons Learned from Recent Strong Earthquakes". Istanbul, Turkey.

Yasuda, S. (2004). Chapter 6 Evaluation of liquefaction-induced deformation of structures. 199-230. Recent advances in earthquake geotechnical engineering and microzonation. Ed. Ansal, A. Kluwer Academic Publishers.

Youd, T.L., Idriss, I.M., Andrus, R.D., Arango, I., Castro, G., Christian, J.T., Dobry, R. Finn, W.D.L., Harder, L.F. Jr., Hynes, M.E., Ishihara, K., Koester, J.P., Liao, S.S.C., Marcuson III, W.F., Martin, G.R., Mitchell, J.K., Moriwaki, Y., Power, M.S., Robertson, P.K., Seed, R.B. and Stokoe II, K.H.(2001). Liquefaction Resistance of Soils: Summary Report from the 1996 NCEER and 1998 NCEER/NSF Workshops on Evaluation of Liquefaction Resistance of Soils. *Journal of Geotechnical and Geoenvironmental Engineering*.**127:10**. 817-833